Determining Biomembrane Bending Rigidities from Simulations of Modest Size

Max C. Watson,[1] Erik G. Brandt,[2,3] Paul M. Welch,[4] and Frank L. H. Brown[1,3]

[1]*Department of Physics, University of California, Santa Barbara, California 93106, USA*
[2]*Department of Mathematics, University of California, Santa Barbara, California 93106, USA*
[3]*Department of Chemistry and Biochemistry, University of California, Santa Barbara, California 93106, USA*
[4]*Theoretical Division, Los Alamos National Laboratory, Los Alamos, New Mexico 87545, USA*

(Received 27 April 2012; published 10 July 2012)

Thermal fluctuations of lipid orientation are analyzed to infer the bending rigidity of lipid bilayers directly from molecular simulations. Compared to the traditional analysis of thermal membrane undulations, the proposed method is reliable down to shorter wavelengths and allows for determination of the bending rigidity using smaller simulation boxes. The requisite theoretical arguments behind this analysis are presented and verified by simulations spanning a diverse range of lipid models from the literature.

DOI: 10.1103/PhysRevLett.109.028102 PACS numbers: 87.16.dj, 46.70.Hg, 87.14.Cc, 87.16.dm

The mechanics of biomembrane shape are commonly formulated in the Helfrich-Canham picture [1–4], which models membranes as thin, structureless, and homogeneous fluid sheets. In the tensionless state, the free energy of such a membrane reads

$$F = \int \left\{ \frac{K_c}{2}(J - C_0)^2 + K_G K \right\} d\mathbf{S}, \tag{1}$$

where J is the local total curvature, K is the local Gaussian curvature, and the integral spans the membrane surface $\mathbf{S}$. The physical constants K_c (bending rigidity), C_0 (spontaneous curvature), and K_G (Gaussian bending rigidity) determine membrane behavior within this picture. For a given surface topology, the second term is a simple constant [5] and $C_0 = 0$ for a symmetric bilayer with identical leaflets. This leaves K_c to fully specify membrane behavior and to distinguish between chemically distinct membranes for many common experiments (within the Helfrich-Canham model). The membrane's resistance to bending plays an important role in a number of biological situations, including endocytosis [6], the organization of membrane trafficking [7], and membrane fusion [8]. K_c is arguably the single most important quantity in membrane biophysics, and considerable effort has been expended on measuring, predicting, and understanding how it varies across different lipid bilayers [4,9–18].

Analyzing thermal shape fluctuations of tensionless quasiplanar membranes in a periodic simulation box [18–20] has become the standard method for determining K_c from molecular simulations. In this geometry, the Helfrich-Canham surface is conveniently specified by the "height field" $h(x, y) = h(\mathbf{r})$, which indicates the vertical displacement of the membrane from the minimum energy configuration $h(\mathbf{r}) = 0$. Equation (1) may then be written, assuming small deviations from $h(\mathbf{r}) = 0$, as $F = \frac{K_c}{2}\int_{L^2}(\nabla^2 h)^2 d\mathbf{r}$ or $F = \frac{K_c}{2}\sum_{\mathbf{q}} q^4 |h_{\mathbf{q}}|^2$ for $h(\mathbf{r}) = \frac{1}{L}\sum_{\mathbf{q}} h_{\mathbf{q}} e^{i\mathbf{q}\cdot\mathbf{r}}$ expressed as a Fourier series. The equipartition theorem then predicts $\langle |h_{\mathbf{q}}|^2 \rangle = k_B T / K_c q^4$; the value of K_c is inferred by fitting the simulation results for $\langle |h_{\mathbf{q}}|^2 \rangle$ to this expression.

Schemes to extract K_c from simulation data by analyzing membrane response to applied forces have also been proposed [21–23]. These methods are interesting from theoretical and conceptual perspectives and have helped to demonstrate the validity of Eq. (1) over a range of geometries, but are not widely used as practical tools to extract K_c from simulations. The overwhelming popularity of the shape fluctuation approach follows from the straightforward nature of both the required simulations and subsequent analysis, as well as the generality of the approach to a diverse range of membrane models spanning coarse-grained to fully atomic representations. The other schemes are more complicated to implement and/or may be well suited only for simplified lipid representations.

Despite widespread use of the shape fluctuation methodology, the approach is open to criticism. The underlying theory [Eq. (1)] presumes that the membrane is a thin sheet devoid of any internal structure. While this assumption holds for fluid bilayers over sufficiently long wavelengths, it necessarily breaks down at length scales comparable to the bilayer thickness. Due to computational constraints, simulations often involve a membrane patch that is only on the order of ten times larger in lateral dimension than the membrane is thick. It is not obvious that Eq. (1) should hold at these length scales; indeed, the prediction $\langle |h_{\mathbf{q}}|^2 \rangle = k_B T / K_c q^4$ is seldom a perfect fit to the simulation data, even at the longest wavelengths allowed by the box (e.g., see Fig. 5). This imperfect correspondence between theory and experiment at observable wavelengths is, at least partially, to blame for the disparity of reported values of K_c for identical simulation models [20,24–28]. Recent theories [26,29,30], which include the influence of lipid tilt on bilayer shape [31,32], have provided improved predictions for $\langle |h_{\mathbf{q}}|^2 \rangle$ over simulated length scales, but we argue that the focus on $\langle |h_{\mathbf{q}}|^2 \rangle$ is primarily motivated by history and may be somewhat misguided. A more lucid physical

picture, simpler theoretical expressions and streamlined data analysis are suggested by concentrating interest on fluctuations in lipid orientation.

In this Letter, we demonstrate that K_c can be measured by directly analyzing thermal fluctuations in lipid orientation. This approach is similar to methods that have been applied to determine Frank elastic constants in the liquid crystal literature (see [33] and references therein). The method relies on identical simulations and similar analyses as employed in the shape fluctuation approach, but has the advantage that theory and simulation show good agreement down to shorter wavelengths. This makes it possible to determine K_c for detailed lipid models more accurately than was previously possible. Existing simulation data may be re-analyzed to obtain better estimates of K_c without the need to perform new simulations. Insofar as K_c provides a key physical observable to compare theory, experiment, and simulation in membrane biophysics, this represents an important practical step forward in our understanding of these systems. In addition to K_c, the technique provides a straightforward method for measuring the lipid tilt modulus K_θ and twist modulus K_{tw}, which govern mesoscopic aspects of bilayer structure.

Our theoretical approach is based on a reformulation of the model described in Ref. [26], by changing basis within the theory to replace the bilayer height field with the longitudinal component of the vector field associated with lipid orientation. Those aspects of the original theory needed to motivate this reformulation are summarized here. We refer readers to Ref. [26] for a detailed explanation and derivation of the model itself. Here, we focus only on the smooth "macroscopic" contributions to bilayer energetics and ignore microscopic "protrusions." Our intent is to provide a practical scheme to extract K_c from simulation data, and we demonstrate that the macroscopic model alone is sufficient to accomplish this. Readers interested in the protrusion regime are referred to Ref. [26].

The geometric setup of the model is illustrated in Fig. 1, adopting the notation of Ref. [26]. The superscript $\alpha = \{1, 2\}$ refers to the top and bottom leaflets, respectively. The font $\mathbb{n}$ denotes a 3D vector, while $\mathbf{n}$ denotes its xy components. The vector $\mathbf{r}$ refers to xy position. We denote the exact bilayer height field as $h(\mathbf{r})$, while $z^+(\mathbf{r})$ denotes the smooth macroscopic continuum field used to approximate h in the absence of protrusions. From the definitions described in Fig. 1, it is convenient to use the quantities $\hat{\mathbf{n}} \equiv \frac{1}{2}[\mathbf{n}^{(1)} - \mathbf{n}^{(2)}]$ and $\hat{\mathbf{m}} \equiv \frac{1}{2}[\mathbf{m}^{(1)} - \mathbf{m}^{(2)}]$ to describe the collective molecular orientation and tilt of the bilayer, respectively.

The bilayer free energy decouples into independent peristaltic modes, which correspond to perturbations in bilayer thickness, and undulation modes, which are associated with overall membrane shape. In this Letter, we are only concerned with undulations. For vanishing surface tension and fixed topology, the free energy associated with undulations is [see Eqs. (18) and (20) of Ref. [26]]

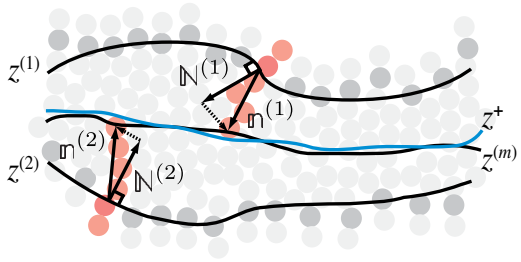

FIG. 1 (color online). For each leaflet, $z^{(\alpha)}$ represents the smooth (protrusionless) surface running though the hydrocarbon water surfaces. $z^{(m)}$ is the smooth surface which separates the top and bottom leaflets, so that the top monolayer is bounded by $z^{(1)}$ and $z^{(m)}$, while the bottom monolayer is bounded by $z^{(m)}$ and $z^{(2)}$. The coarse-grained shape of the membrane averaged over the top and bottom monolayers is given by $z^+ \equiv \frac{1}{2}[z^{(1)} + z^{(2)}]$. The unit vectors $\mathbb{N}^{(\alpha)}$ are normal to $z^{(\alpha)}$ and point toward the interior of the bilayer. Assuming the membrane is nearly flat, the normals may be approximated as $\mathbb{N}^{(\alpha)} = (-1)^\alpha[-\nabla z^{(\alpha)}, 1]$. Molecular orientation of the lipids is described by the unit vector field $\mathbb{n}^{(\alpha)}$, which points from $z^{(\alpha)}$ to $z^{(m)}$ along a vector connecting the two ends of the lipid hydrocarbon chain(s). The xy components of the dashed vectors denote the tilt vector $\mathbf{m}^{(\alpha)} = \mathbf{n}^{(\alpha)} - \mathbf{N}^{(\alpha)}$.

$$F_u = \frac{1}{2}\int\Big(K_c^b(\nabla^2 z^+ + \nabla\cdot\hat{\mathbf{m}})^2 - \frac{\tilde{\Omega}}{b_0}\varepsilon(\nabla^2 z^+ + \nabla\cdot\hat{\mathbf{m}}) + \frac{K_A}{b_0^2}\varepsilon^2 + K_\theta\hat{\mathbf{m}}^2 + K_{\mathrm{tw}}(\nabla\times\hat{\mathbf{m}})^2\Big)d\mathbf{r}, \quad (2)$$

where $\varepsilon \equiv z^{(m)} - z^+$ and b_0 is the mean monolayer thickness. The elastic moduli in Eq. (2): K_c^b (bending modulus for constant monolayer thickness deformations), K_A (compressibility modulus), K_θ (tilt modulus), K_{tw} (twist modulus), and $\tilde{\Omega}$ (bending-compression coupling) represent bilayer quantities and are twice the corresponding monolayer quantities introduced in Ref. [26] (e.g., $K_A = 2k_A$, etc.).

Due to coupling between z^+, ε, and $\hat{\mathbf{m}}$, K_c^b is not the quantity associated with bilayer bending in the usual sense. $K_c = K_c^b - \tilde{\Omega}^2/8K_A$ has all the properties usually associated with the bilayer bending modulus [26]. In particular, $\langle|z_{\mathbf{q}}^+|^2\rangle = k_BT/K_cq^4$ asymptotically as $q \to 0$ for this model [26]. In this regime, the details of internal structure within the bilayer are unimportant, and membrane shape behaves as predicted by the Helfrich-Canham picture. However, the general prediction following from Eq. (2) is [26]

$$\langle|z_{\mathbf{q}}^+|^2\rangle = k_BT\left(\frac{1}{K_cq^4} + \frac{1}{K_\theta q^2}\right). \quad (3)$$

The second term reflects energetic coupling between shape and tilt (see Fig. 2), and is an important contribution to $\langle|z_{\mathbf{q}}^+|^2\rangle$ on length scales comparable to and somewhat larger than the bilayer thickness [29,30] (see Fig. 5). (An additive q^{-2} contribution to the traditional height spectrum was originally proposed in Ref. [18], and was attributed to microscopic protrusions. Simultaneous analysis of membrane shape and lipid tilting in molecular simulations indicates

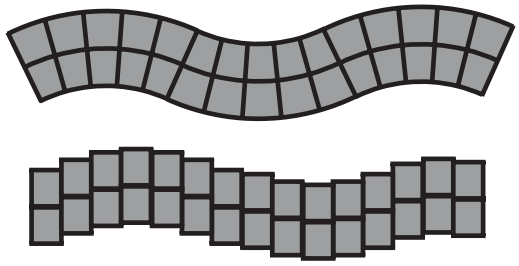

FIG. 2. Two modes of membrane bending (each box represents a lipid and $\varepsilon = 0$ for simplicity). Top: Membrane bending associated with splay in lipid orientation ($\nabla \cdot \hat{\mathbf{n}}$), in the absence of any lipid tilting ($\hat{\mathbf{m}}$). Bottom: Membrane bending associated with lipid tilt, in the absence of splay. The top mode represents the dominant contribution to bending at long wavelengths and the source of q^{-4} scaling in $\langle |h_{\mathbf{q}}|^2 \rangle$. The bottom mode involves an increase in the average area per lipid exposed to solvent and is associated with a q^{-2} scaling characteristic shape fluctuations damped by surface tension.

that q^{-2} scaling at short wavelengths is primarily attributable to lipid tilt [26,29].)

Equation (2) simplifies by recognizing that $\hat{\mathbf{n}} = \nabla z^+ + \hat{\mathbf{m}}$, so that the free energy may be rewritten as

$$F_u = \frac{1}{2}\int\Big(K_c^b(\nabla\cdot\hat{\mathbf{n}})^2 - \frac{\tilde{\Omega}}{b_0}\varepsilon\nabla\cdot\hat{\mathbf{n}} + \frac{K_A}{b_0^2}\varepsilon^2 + K_\theta\hat{\mathbf{m}}^2 + K_{tw}(\nabla\times\hat{\mathbf{m}})^2\Big)d\mathbf{r}. \quad (4)$$

This change amounts to a simple linear transformation to express the energy in a form that is almost diagonal and displays similarity to the Frank theory of nematic liquid crystals [31,32,34] at the expense of losing explicit reference to the shape field z^+ familiar from Helfrich-Canham theory. The two representations [Eqs. (2) and (4)] are completely equivalent within the quadratic order expansion in small quantities implicit in the theoretical treatment.

Thermal fluctuation spectra are calculated from Eq. (4) as follows. For a box with periodic boundary conditions and area L^2, we adopt the Fourier representation discussed earlier. The values of the wave number $\mathbf{q}$ are given by $\mathbf{q} = 2\pi(n,m)/L$ for the integers $n, m = \{-\frac{M}{2}, \ldots, 0, \ldots, \frac{M}{2} - 1\}$, where M is dictated by a short wavelength cutoff. $\hat{\mathbf{n}}_{\mathbf{q}}$ may be written in terms of longitudinal and transverse components $\hat{n}_{\mathbf{q}}^{\parallel} = \frac{1}{q}[\mathbf{q}\cdot\hat{\mathbf{n}}_{\mathbf{q}}]$ and $\hat{n}_{\mathbf{q}}^{\perp} = \frac{1}{q}[\mathbf{q}\times\hat{\mathbf{n}}_{\mathbf{q}}]\cdot\hat{z}$, and similarly for $\hat{\mathbf{m}}$. In Fourier space, the energy reads $F_u = \frac{1}{2}\sum_{\mathbf{q}}\tilde{\mathbf{f}}_u(-\mathbf{q})\otimes\mathbf{C}\otimes\tilde{\mathbf{f}}_u^T(\mathbf{q})$, where $\tilde{\mathbf{f}}_u(\mathbf{q}) = [\hat{n}_{\mathbf{q}}^{\parallel}, \varepsilon_{\mathbf{q}}, \hat{m}_{\mathbf{q}}^{\parallel}, \hat{m}_{\mathbf{q}}^{\perp}]$ and

$$\mathbf{C} = \begin{pmatrix} K_c^b q^2 & iq\tilde{\Omega}/b_0 & 0 & 0 \\ -iq\tilde{\Omega}/b_0 & K_A/b_0^2 & 0 & 0 \\ 0 & 0 & K_\theta & 0 \\ 0 & 0 & 0 & K_\theta + K_{\mathrm{tw}}q^2 \end{pmatrix}.$$

From the equipartition theorem [3], thermal fluctuations in lipid orientation follow immediately:

$$\langle|\hat{n}_{\mathbf{q}}^{\parallel}|^2\rangle = \frac{k_BT}{K_cq^2}, \qquad \langle|\hat{n}_{\mathbf{q}}^{\perp}|^2\rangle = \frac{k_BT}{K_\theta + K_{tw}q^2}. \quad (5)$$

The first of these equations represents the primary result of this Letter, establishing a foundation for determination of K_c directly from fluctuations in the longitudinal component of lipid orientation. The second equation follows from the fact that $\hat{n}_{\mathbf{q}}^{\perp} = \hat{m}_{\mathbf{q}}^{\perp}$ since $\hat{\mathbf{n}} = \nabla z^+ + \hat{\mathbf{m}}$. From Eq. (5), the tilt and twist moduli $\{K_\theta, K_{tw}\}$ may be extracted from the transverse orientation fluctuations.

The theoretical predictions were compared against three very different molecular simulations: an aggressively coarse-grained implicit solvent system (CG) [25], the MARTINI model for DPPC [27,35], and a united atom (UA) force field for DMPC [36]. Trajectories from previously reported simulations [24,26] were used in the analysis. We are unaware of the quantities $\langle|\hat{n}_{\mathbf{q}}^{\parallel}|^2\rangle$ and $\langle|\hat{n}_{\mathbf{q}}^{\perp}|^2\rangle$ previously being measured in simulations, but closely related tilt fluctuations have been reported [26,29,30]. Appendix C of Ref. [26] details the analysis of molecular simulation trajectories to obtain tilt, height, and related fluctuation spectra. This procedure was adapted to measure orientation spectra simply by considering the molecular orientation vectors directly, without subtracting off the local shape gradients ($\nabla z^{(\alpha)}$) needed in the definition of tilt. The only ambiguity in the process lies in defining the orientation for individual lipids. (Where do you place the vector head and tail relative to the atoms or sites in the molecule?) The data presented in Figs. 3–5 assume the following definitions: for the UA model, the molecular orientation of each lipid [i.e., $\mathbb{n}^{(\alpha)}$ for that lipid] points from the phosphate atom to the midpoint between the last carbons of the two hydrocarbon chains; for the implicit solvent system and MARTINI model, the vector points from the interfacial beads to the last tail beads of the chains (see Fig. 7 of Ref. [26]).

In order to extract K_c, the raw data for $\langle|\hat{n}_{\mathbf{q}}^{\parallel}|^2\rangle$ is multipled by q^2 (Fig. 3). As predicted by Eq. (5), these scaled data are constant until microscopic fluctuations (e.g., protrusions) become prominent at short wavelengths. The values of K_c were obtained by taking the average of the data points over wavelengths greater than twice the bilayer thickness, yielding $K_c = \{36, 15, 15\} \times 10^{-20}$ J for the CG, MARTINI, and UA models, respectively. The first two values agree with previous measurements [26,28]. K_c obtained for the UA DMPC model is twice as large as a recently reported value [24] based on exactly the same simulation run as this paper. The disparity is due to a subtle difference [37] associated with the "direct Fourier" analysis method proposed and employed to analyze the simulation in Ref. [24]. (The experimentally measured value of K_c for DMPC ranges from 15×10^{-20} J [38,39] to roughly half that number [10,40].) The analysis was repeated using different

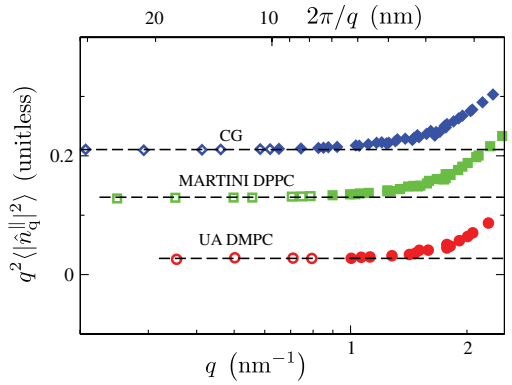

FIG. 3 (color online). The spectrum of longitudinal molecular orientation fluctuations $\langle|\hat{n}_\mathbf{q}^\parallel|^2\rangle$ multipled by q^2. Simulation data are shown for an implicit solvent model (CG) (◇), the MARTINI model for DPPC (□), and a united-atom force field for DMPC (○). Open symbols denote wavelengths greater than twice the bilayer thickness, used in determination of K_c. For clarity, the data sets for MARTINI and CG were vertically shifted by 0.1 and 0.2, respectively.

definitions for the molecular orientation vector, as suggested in Refs. [29,30] (data not shown). The extracted values of K_c changed by 5% or less. This degree of influence on K_c is similar to that found by changing the molecular definition of $z^{(\alpha)}$ in the traditional shape analysis.

The tilt and twist moduli $\{K_\theta, K_{\mathrm{tw}}\}$ were obtained by fitting the transverse fluctuations to Eq. (5) over all values of q. The results are shown in Fig. 4. The fitted values are $K_\theta = \{5.2, 11, 5.6\} \times 10^{-20} \frac{\mathrm{J}}{\mathrm{nm}^2}$ and $K_{\mathrm{tw}} = \{2.2, 1.5, 2.4\} \times 10^{-20}$ J for the CG, MARTINI, and UA models, respectively. Unlike K_c, the values of $\{K_\theta, K_{\mathrm{tw}}\}$ are more sensitive to the molecular definition of orientation [29,30].

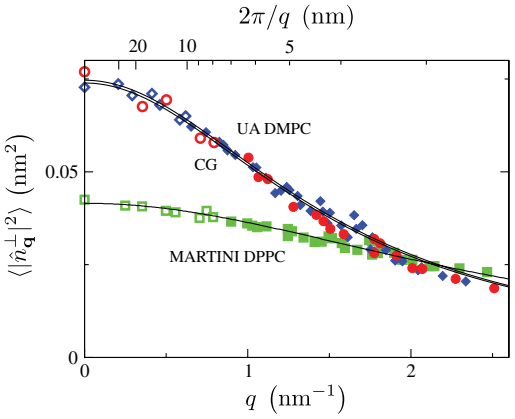

FIG. 4 (color online). The transverse orientation spectrum $\langle|\hat{n}_\mathbf{q}^\perp|^2\rangle$ (see Fig. 3 for details). In contrast to $\langle|\hat{n}_\mathbf{q}^\parallel|^2\rangle$, the theory (solid lines) and simulation data agree down to wavelengths of a few nanometers [Eq. (5)]. While different definitions of the molecular orientation lead to quantitative changes in the $\langle|\hat{n}_\mathbf{q}^\perp|^2\rangle$ data for MARTINI and UA, the resulting spectra (not shown) retain excellent agreement with Eq. (5).

We find $K_\theta = 9 \times 10^{-20} \frac{\mathrm{J}}{\mathrm{nm}^2}$ for the MARTINI model when choosing the midpoints of all head beads and tail beads to represent the start points and endpoints of $\mathbb{n}^{(\alpha)}$, respectively. For UA, $K_\theta = 3.6 \times 10^{-20} \frac{\mathrm{J}}{\mathrm{nm}^2}$ when drawing $\mathbb{n}^{(\alpha)}$ from the carbon joining the two chains to the midpoint of the carbons at the end of each chain (data not shown).

For purposes of comparison, we plot $\langle|h_\mathbf{q}|^2\rangle q^4$ for the same three simulations in Fig. 5. If the traditional Helfrich-Canham prediction held, we could extract the bending modulus as $K_c = k_B T/[\langle|h_\mathbf{q}|^2\rangle q^4]$ in the regime where the denominator is constant. This regime is, at best, confined to the longest two wavelength modes for both the CG and MARTINI data; it is not present at all for the UA model. It is difficult to see how one could be confident with a K_c value extracted in this manner, for any of these simulations. An improved analysis to obtain K_c from the height field is possible, but requires use of Eq. (3) and knowledge of K_θ (see Fig. 5). Using the values of K_θ determined from the transverse orientation fluctuations in Fig. 4, we find $K_c = \{37, 14, 11\} \times 10^{-20}$ J for the CG, MARTINI, and UA models. However, repeating the analysis with the alternate orientation definitions discussed above leads to $K_c = \{13, 16\} \times 10^{-20}$ J for the MARTINI and UA models. Unfortunately, the sensitivity of K_θ to the molecular definition of orientation propagates to uncertainty in K_c when using this approach. No such uncertainty exists for the analysis based on the longitudinal orientation fluctuations. The need to introduce K_θ to solve for K_c is a considerable disadvantage. Figure 5 is intended to demonstrate the consistency of the underlying theoretical treatment and to highlight shortcomings of the traditional approach, not to suggest determination of K_c via height fluctuations.

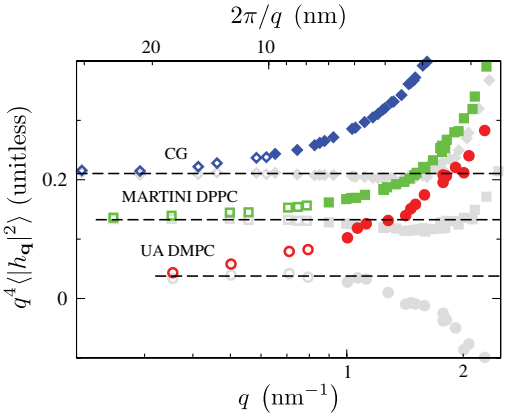

FIG. 5 (color online). The spectrum of height fluctuations $\langle|h_\mathbf{q}|^2\rangle$ multiplied by q^4 for the same simulations as in Fig. 3. The gray symbols represent "correcting" these results, as suggested by Eq. (3), to account for lipid tilt: $[\langle|h_\mathbf{q}|^2\rangle - \frac{k_B T}{K_\theta q^2}]q^4$. For clarity, the MARTINI and CG data sets were vertically shifted by 0.1 and 0.2, respectively.

The primary message of this Letter may be seen in the contrast between Figs. 3 and 5. If the Helfrich-Canham theory were sufficient to describe membrane mechanics over the scales probed in molecular simulations, both figures would exhibit a significant plateau regime at low wave numbers. In practice, such behavior is observed only in Fig. 3, indicating the influence of lipid tilting on the height spectrum. Lipid splay ($\nabla \cdot \hat{\mathbf{n}}$) is the only microscopic deformation responsible for macroscopic bending, as tilting is relatively unfavorable over long wavelengths (Fig. 2). Splay is associated with the longitudinal component of the lipid orientation field and Eq. (5) provides a simple means to extract K_c from molecular simulations based on this fact. As a practical matter, the proposed method for measuring K_c can be applied to simulations smaller than the ones used here and smaller than is needed to determine K_c based on the popular shape fluctuation approach. For the united atom simulation, a minimum wave number of about 0.6 nm^{-1} could have been used to safely measure the bending modulus (Figs. 3 and 5). Based on the area per molecule of 0.6 nm^2, a system consisting of $\sim$400 lipids would be sufficient. This suggests that it may be possible to accurately and routinely determine K_c for various lipid systems, even fully-atomic models. Due to its straightforward measurement, the orientation spectra should join the list of standard quantities used to characterize lipid simulations.

Partial financial support was provided by the Los Alamos National Laboratory Institute for Multiscale Materials Studies, operated under the auspices of the National Nuclear Security Administration of the U.S. Department of Energy under Contract No. DE-AC52-06NA25396. This work is partially supported by the NSF (CHE-0848809, CHE-1153096, CNS-0960316). E. G. B. acknowledges support from the Kozato Fund. F. L. H. B. acknowledges support from the Camille and Henry Dreyfus Foundation. We thank Olle Edholm for the UA simulation trajectory.

[1] W. Helfrich, Z. Naturforsch. **28C**, 693 (1973).
[2] P. B. Canham, J. Theor. Biol. **26**, 61 (1970).
[3] S. A. Safran, *Statistical Thermodynamics of Surfaces, Interfaces and Membranes* (Westview Press, Boulder, CO, 1994).
[4] D. H. Boal, *Mechanics of the Cell* (Cambridge University Press, Cambridge, 2002).
[5] R. D. Kamien, Rev. Mod. Phys. **74**, 953 (2002).
[6] J. Liu, M. Kaksonen, D. G. Drubin, and G. Oster, Proc. Natl. Acad. Sci. U.S.A. **103**, 10277 (2006).
[7] H. T. McMahon and J. L. Gallop, Nature (London) **438**, 590 (2005).
[8] L. Chernomordik, M. Kozlov, and J. Zimmerberg, J. Membr. Biol. **146**, 1 (1995),
[9] R. Lipowsky and E. Sackmann, *Structure and Dynamics of Membranes* (North Holland, Amsterdam, 1995).
[10] W. Rawicz, K. Olbrich, T. McIntosh, D. Needhamand, and E. Evans, Biophys. J. **79**, 328 (2000).
[11] Z. Yi, M. Nagao, and D. Bossev, J. Phys. Condens. Matter **21**, 155104 (2009).
[12] M. F. Brown, R. L. Thurmond, S. W. Dodd, D. Otten, and K. Beyer, J. Am. Chem. Soc. **124**, 8471 (2002).
[13] P. Méléard, C. Gerbeaud, T. Pott, L. Fernandez-Puente, I. Bivas, M. Mitov, J. Dufourcq, and P. Bothorel, Biophys. J. **72**, 2616 (1997).
[14] E. Evans, Biophys. J. **43**, 27 (1983).
[15] L. Bo and R. E. Waugh, Biophys. J. **55**, 509 (1989).
[16] R. Simson, E. Wallraff, J. Faix, J. Niewöhner, G. Gerisch, and E. Sackmann, Biophys. J. **74**, 514 (1998).
[17] T. Baumgart, S. Das, W. Webb, and J. Jenkins, Biophys. J. **89**, 1067 (2005).
[18] R. Goetz, G. Gompper, and R. Lipowsky, Phys. Rev. Lett. **82**, 221 (1999).
[19] S. J. Marrink and A. E. Mark, J. Phys. Chem. **105**, 6122 (2001).
[20] E. Lindahl and O. Edholm, Biophys. J. **79**, 426 (2000).
[21] W. K. den Otter and W. J. Briels, J. Chem. Phys. **118**, 4712 (2003).
[22] O. Farago and P. Pincus, J. Chem. Phys. **120**, 2934 (2004).
[23] V. A. Harmandaris and M. Deserno, J. Chem. Phys. **125**, 204905 (2006).
[24] E. G. Brandt, A. R. Braun, J. N. Sachs, J. F. Nagle, and O. Edholm, Biophys. J. **100**, 2104 (2011).
[25] G. Brannigan, P. F. Phillips, and F. L. H. Brown, Phys. Rev. E **72**, 011915 (2005).
[26] M. C. Watson, E. S. Penev, P. M. Welch, and F. L. H. Brown, J. Chem. Phys. **135**, 244701 (2011).
[27] S. J. Marrink, A. H. de Vries, and A. E. Mark, J. Phys. Chem. B **108**, 750 (2004).
[28] S. Shkulipa, Ph.D. thesis, University of Twente, 2006.
[29] E. R. May, A. Narang, and D. I. Kopelevich, Phys. Rev. E **76**, 021913 (2007).
[30] E. R. May, A. Narang, and D. I. Kopelevich, Mol. Simul. **33**, 787 (2007).
[31] M. Hamm and M. M. Kozlov, Eur. Phys. J. E **6**, 519 (1998).
[32] M. Hamm and M. M. Kozlov, Eur. Phys. J. E **3**, 323 (2000).
[33] N. H. Phuong, G. Germano, and F. Schmid, J. Chem. Phys. **115**, 7227 (2001).
[34] F. C. Frank, Discuss. Faraday Soc. **25**, 19 (1958).
[35] S. J. Marrink, J. H. Risselada, S. Yefimov, P. D. Tieleman, and A. H. de Vries, J. Phys. Chem. B **111**, 7812 (2007).
[36] O. Berger, O. Edholm, and F. Jähnig, Biophys. J. **72**, 2002 (1997).
[37] E. G. Brandt, M. C. Watson, P. J. Atzberger, and F. L. H. Brown (to be published).
[38] C.-H. Lee, W. C. Lin, and J. Wang, Phys. Rev. E **64**, 020901 (2001).
[39] H. Duwe and E. Sackmann, Physica (Amsterdam) **163A**, 410 (1990).
[40] N. Kučerka, Y. Liu, N. Chu, H. I. Petrache, S. Tristram-Nagle, and J. F. Nagle, Biophys. J. **88**, 2626 (2005).